Cyclic Voltammetric Characterization of Rate Constants for Conformational Change in an Electron-Transfer Square Scheme Involving a Copper(II)/(I) Macrocyclic Tetrathiaether Complex

Paul V. Robandt, Ronald R. Schroeder,* and D. B. Rorabacher*

Department of Chemistry, Wayne State University, Detroit, Michigan 48202

Received March 23, 1993

With a glassy-carbon ultramicroelectrode and appropriate circuitry, cyclic voltammograms have been generated for solutions containing the $Cu^{II/I}([14]aneS_4)$ system at scan rates up to 60 kV s^{-1} in 80% methanol (w/w) at 25 °C. These rapid-scan voltammograms provide direct evidence for the existence of metastable intermediates of both the $Cu^{I}L$ and the $Cu^{II}L$ species in conformance with our previously proposed square scheme mechanism. On the basis of the experimental data, estimates have been made for all the specific homogeneous and heterogeneous rate constants associated with this square scheme. The values of these constants have then been further refined using digital simulation. The resulting simulated voltammograms are shown to correlate reasonably well with the experimental observations at even the most rapid scan rates achieved. The availability of the specific rate constant values representing $Cu^{I}L$ and $Cu^{II}L$ conformational interconversions makes it possible to predict the conditions under which conformational change of the $Cu^{I}L$ species should become rate limiting, resulting in the appearance of gated electron-transfer behavior in homogeneous cross reactions.

Introduction

Conformational constraints upon the active site have long been recognized as an important factor in controlling the reactivity of biological enzymes, particularly in the case of redox-active metalloenzymes involving iron and copper.[1] Only recently, however, has it become evident that the rate of conformational change may itself become the rate-limiting step in the reactions of the heme proteins, cytochrome *c* oxidase, and other biologically important iron and copper systems.[2-10] This implies that the electron-transfer step and the relevant conformational alterations occurring during such electron-transfer processes are sequential rather than concerted, resulting in the generation of conformational intermediates for both the oxidized and reduced species.[11-14]

During the past decade and a half, much attention has been devoted to the chemistry of the blue copper proteins, particularly those species containing a single type 1 copper site (sometimes known as the blue electron carriers) including plastocyanin, azurin, stellacyanin, rusticyanin, and others, of which the first two are the most extensively studied.[15-22] Although the structural features in the vicinity of the copper atom appear to be similar in both the oxidized and reduced enzymes,[16] several pieces of experimental evidence indicate that the copper sites may not be as rigid as implied by the crystal structures. Limiting first-order kinetics have been observed in bimolecular reactions for the reduction of rusticyanin[23] and the oxidation of azurin.[24,25] This behavior has been attributed to rate-limiting conformational changes at the copper site preceding the electron-transfer step. Furthermore, for both rusticyanin and azurin, spectral evidence has been obtained for the existence of two conformers of the copper site.[23,26] To date, however, it has not been possible to characterize these individual conformers thoroughly, nor has direct evaluation of the rate constants governing the conformational interconversions been reported.

In studies within our own laboratory,[27-29] we have found evidence for similar conformational changes occurring in a series of low molecular weight copper complexes formed with cyclic

(1) (a) Vallee, B. L.; Williams, R. J. P. *Proc. Natl. Acad. Sci. U.S.A.* **1968**, *59*, 498–505. (b) Williams, R. J. P. *Inorg. Chim. Acta Rev.* **1971**, *5*, 137–155.
(2) Bechtold, R.; Kuehn, C.; Lepre, C.; Isied, S. S. *Nature* **1986**, *322*, 286–288.
(3) Feitelson, J.; McLendon, G. *Biochemistry* **1991**, *30*, 5051–5055.
(4) Malmstrom, B. G.; Nilsson, T. *Ann. N.Y. Acad. Sci.* **1988**, *550*, 177–184.
(5) Nocek, J. M.; Liang, N.; Wallin, S. A.; Mauk, A. G.; Hoffman, B. M. *J. Am. Chem. Soc.* **1990**, *112*, 1623–1625.
(6) Wilson, M. T.; Alleyne, T.; Clague, M.; Conroy, K.; El-Agez, B. *Ann. N.Y. Acad. Sci.* **1988**, *550*, 167–176.
(7) Zang, L.-H.; Maki, A. H. *J. Am. Chem. Soc.* **1990**, *112*, 4346–4351.
(8) Isied, S. S. In *Electron Transfer in Biology and the Solid State*; Johnson, M. K., King, R. B., Kurtz, D. M., Jr., Kutal, C., Norton, M. L., Scott, R. A., Eds.; Advances in Chemistry 226; American Chemical Society: Washington, DC, 1990; pp 91–100.
(9) Walker, M. C.; Tollin, G. *Biochemistry* **1991**, *30*, 5546–5555.
(10) Wallin, S. A.; Stemp, E. D. A.; Everest, A. M.; Nocek, J. M.; Netzel, T. L.; Hoffman, B. M. *J. Am. Chem. Soc.* **1991**, *113*, 1842–1844.
(11) Hoffman, B. M.; Ratner, M. A. *J. Am. Chem. Soc.* **1987**, *109*, 6237–6243; **1988**, *110*, 8267.
(12) Hoffman, B. M.; Ratner, M. A.; Wallin, S. A. In *Electron Transfer in Biology and the Solid State*; Johnson, M. K., King, R. B., Kurtz, D. M., Jr., Kutal, C., Norton, M. L., Scott, R. A., Eds.; Advances in Chemistry 226; American Chemical Society: Washington, DC, 1990; pp 125–146.
(13) Brunschwig, B. S.; Sutin, N. *J. Am. Chem. Soc.* **1989**, *111*, 7454–7465.
(14) Sutin, N.; Brunschwig, B. S. In *Electron Transfer in Biology and the Solid State*; Johnson, M. K., King, R. B., Kurtz, D. M., Jr., Kutal, C., Norton, M. L., Scott, R. A., Eds.; Advances in Chemistry 226; American Chemical Society: Washington, DC, 1990; pp 65–88.
(15) Colman, P. M.; Freeman, H. C.; Guss, J. M.; Murata, M.; Norris, V. A.; Ramshaw, J. A. M.; Venkatappa, M. P. *Nature* **1978**, *272*, 319–324.
(16) Guss, J. M.; Freeman, H. C. *J. Mol. Biol.* **1983**, *169*, 521–563. Cf.; Freeman, H. C. In *Coordination Chemistry*; Laurent, J. P., Ed.; Pergamon Press: Oxford, England, 1981; Vol. 21, pp 29–51.
(17) Adman, E. T.; Stenkamp, R. E.; Sieker, L. C.; Jensen, L. H. *J. Mol. Biol.* **1978**, *123*, 35–47.
(18) Adman, E. T.; Jensen, L. H. *Isr. J. Chem.* **1981**, *21*, 8–12.
(19) Norris, G. E.; Anderson, B. F.; Baker, E. N. *J. Mol. Biol.* **1983**, *165*, 501–521.
(20) Baker, E. N. *J. Mol. Biol.* **1988**, *203*, 1071–1095.
(21) Nar, H.; Messerschmidt, A.; Huber, R.; van de Kamp, M.; Canters, G. W. *J. Mol. Biol.* **1991**, *218*, 427–447.
(22) Norris, G. E.; Anderson, B. F.; Baker, E. N. *J. Am. Chem. Soc.* **1986**, *108*, 2784–2785.
(23) Lappin, A. G.; Lewis, C. A.; Ingledew, C. A. *Inorg. Chem.* **1985**, *24*, 1446–1450.
(24) Rosen, P.; Pecht, I. *Biochemistry* **1976**, *15*, 775–786.
(25) (a) Silvestrini, M. C.; Brunori, M.; Wilson, M. T.; Darley-Usmar, V. M. *J. Inorg. Biochem.* **1981**, *14*, 327–338. (b) Mitra, S.; Bersohn, R. *Proc. Natl. Acad. Sci. U.S.A.* **1982**, *79*, 6807–6811.
(26) Szabo, A. G.; Stepanik, T. M.; Wayner, D. M.; Young, N. M. *Biophys. J.* **1983**, *41*, 233–244.
(27) Martin, M. J.; Endicott, J. F.; Ochrymowycz, L. A.; Rorabacher, D. B. *Inorg. Chem.* **1987**, *26*, 3012–3022.
(28) Vande Linde, A. M. Q.; Juntunen, K. L.; Mols, O.; Ksebati, M. B.; Ochrymowycz, L. A.; Rorabacher, D. B. *Inorg. Chem.* **1991**, *30*, 5037–5042.
(29) Bernardo, M. M.; Robandt, P. V.; Schroeder, R. R.; Rorabacher, D. B. *J. Am. Chem. Soc.* **1989**, *111*, 1224–1231.

0020-1669/93/1332-3957$04.00/0

Scheme I

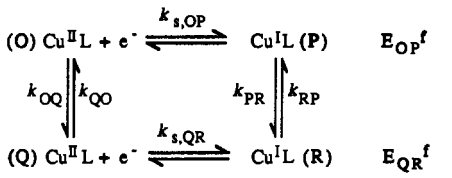

and acyclic polythiaether complexes. These conformational interconversions were first inferred indirectly from their apparent influence upon electron-transfer cross reactions of the type.[27]

$$Cu^{II}L + A_{Red} \underset{k_{21}}{\overset{k_{12}}{\rightleftharpoons}} Cu^{I}L + A_{Ox} \qquad (1)$$

wherein the relevant conformational change either precedes or follows the electron-transfer step, resulting in conformationally-limited electron-transfer behavior under specific conditions. More recently,[29] we were able to obtain direct evidence for the generation of conformational intermediates by using low-temperature cyclic voltammetry to study a specific copper complex, (1,4,8,11-tetrathiacyclotetradecane)copper(II/I)

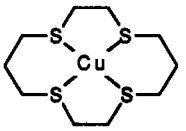

[designated hereafter as $Cu^{II/I}([14]aneS_4)$—or simply $Cu^{II/I}L$] in which the macrocyclic tetrathiaether is capable of square planar or flattened tetrahedral coordination. The voltammetric behavior in 80% methanol-20% water (w/w) was shown to be consistent with the proposed square-scheme mechanism for the coupling of the electron-transfer and conformational changes, as depicted in Scheme I, in which species **O** and **R** represent the stable configurations of $Cu^{II}L$ and $Cu^{I}L$, respectively, while **Q** and **P** are metastable intermediates of these same oxidation states. The rate constants k_{OQ} and k_{QO} are characteristic of the interconversion of the two $Cu^{II}L$ species while k_{PR} and k_{RP} are the corresponding rate constants for the interconversion of the two $Cu^{I}L$ species. The corresponding equilibrium constants are defined as $K_{OQ} = [Q]/[O] = k_{OQ}/k_{QO}$ and $K_{PR} = [R]/[P] = k_{PR}/k_{RP}$.

The previous instrumentation using macroelectrodes[29] was limited to a maximum scan rate of 5–10 V s^{-1}. Under these limiting conditions, observation of the various conformational changes in Scheme I required different temperature domains, including some at temperatures as low as −77 °C. Since the temperature dependencies could not be well established, no attempt was made to evaluate all of the individual rate constants associated with Scheme I other than to provide some very crude estimates which would permit us to demonstrate that the resulting simulated voltammetric curves, based on the foregoing square scheme, could account for all of the various modes of electrochemical behavior observed.

To circumvent the difficulties associated with low-temperature measurements, we have now constructed rapid scan cyclic voltammetric instrumentation and employed a glassy-carbon ultramicroelectrode (5 μm radius) as the working electrode in conjunction with a suitable electrochemical cell and appropriate electronic circuitry. Scan rates of up to 80 kV s^{-1} have been achieved with this setup, permitting a thorough characterization of the $Cu^{II/I}([14]aneS_4)$ system. With the availability of this 10^4-fold increase in scan rate, it has been possible to demonstrate, at a single temperature, all of the limiting features previously observed and/or predicted. This work has also permitted the quantitative evaluation of all four of the rate constants for conformational interconversion (i.e., k_{OQ}, k_{QO}, k_{PR}, and k_{RP}) under uniform conditions. Predictions can now be made regarding the conditions necessary to alter the preferred reaction pathway in homogeneous cross reactions with the $Cu^{II/I}([14]aneS_4)$ system. Such predictions can then be compared to experimental cross reaction measurements to test the efficacy of Scheme I.

Although square scheme electron-transfer behavior has been previously observed for other metal ion complexes[30] (much work in this area having been carried out by Bond and co-workers on systems involving *cis–trans* or *fac–mer* isomerization of metal carbonyl complexes),[31] we know of no previous attempt to evaluate all of the rate constants associated with conformational interconversion for a system involving changes in coordination geometry. Characterization of such rate constants is of particular interest since it has been proposed that, in biological systems, specific conformational or configurational changes may become the rate-limiting step in the overall electron-transfer process, a condition which has been termed "gated"[11] or "directional"[13] electron transfer. In the extreme, the limitations imposed by the rate of conformational change can cause an alteration of the preferred pathway as we have now been able to demonstrate in an independent cross reaction study on the $Cu^{II/I}([14]aneS_4)$ system.[32]

Experimental Section

All cyclic voltammetric data were recorded with a Tektronix 2322 oscilloscope with an 8-bit A/D converter capable of 10^8 samples per second. An averaging algorithm was built into the oscilloscope software. A Tektronix software package, GURU II, was used to download averaged data to a microcomputer via a GPIB interface. A glassy-carbon ultramicrodisk electrode with a radius of 5 μm (Cypress Systems, Lawrence, KS) was used as the working electrode.[33] The surface of this electrode was cleaned each day by wet-sanding it with 600-grade aluminum oxide paper. This was followed by successively polishing with 6-μm diamond paste, 0.3-μm alumina, and 0.05-μm alumina (Buehler, Deerfield, IL) providing a reproducible surface. (The first polishing with diamond paste is the most critical step, requiring up to 10 min.) The electrode was repolished prior to each individual voltammogram with 0.05-μm alumina. Electrochemical pretreatment of the glassy-carbon electrode was not performed for these experiments.

The reference electrode was an aqueous saturated silver/silver chloride electrode (Bioanalytical Systems, West Lafayette, IN) for which $E^f \approx 0.197$ V. The cell consisted of a 250-mL beaker (cut down to reduce the amount of solution required) covered with a Teflon disk with machined holes through which the electrodes could be inserted. The reference electrode was separated from the main compartment by a fritted glass tube of fine porosity. A second fritted glass tube was inserted into the solution for 5 min prior to commencing each experiment to introduce nitrogen for deoxygenation. This tube was then raised above the level of the solution to blanket the cell compartment with nitrogen during the ensuing electrochemical measurements.

Due to the large background current observed at the glassy-carbon electrode, the currents from several runs were first averaged to increase the signal to noise ratio and then a stored background signal was subtracted from the averaged data. The final voltammogram was stored, printed, and plotted. The capacitance of the working electrode was estimated from the magnitude of the charging current in linear sweep experiments and the cell time constant was determined from the charging current decay in single step experiments. The value of the uncompensated resistance was then calculated, and where necessary, positive *iR* drop compensation based on this value was introduced.

To counteract the relatively small stability constant for the $Cu^{II}L$ species, excess aquocopper(II) ion was added to all $Cu^{II}L$ solutions to insure that most of the ligand is in the complexed form. The potential range was generally limited at the high end by the oxidation of the ligand and at the low end by the tendency of the uncomplexed copper(II) ion

(30) Evans, D. H. *Chem. Rev.* **1990**, *90*, 739–751 and references therein.
(31) Bond, A. M.; Colton, R.; Feldberg, S. W.; Mahon, P. J.; Whyte, T. *Organometallics* **1991**, *10*, 3320–3326 and references therein. Cf.: Pramanik, A.; Bag, N.; Ray, D.; Lahiri, K.; Chakravorty, A. *Inorg. Chem.* **1991**, *30*, 410–417.
(32) Meagher, N. E.; Juntunen, K. L.; Salhi, C. A.; Ochrymowycz, L. A.; Rorabacher, D. B. *J. Am. Chem. Soc.* **1992**, *114*, 10411–10420.
(33) Platinum and gold working electrodes were avoided due to the tendency of the tetrathiaether ligand complex to adsorb on these materials.

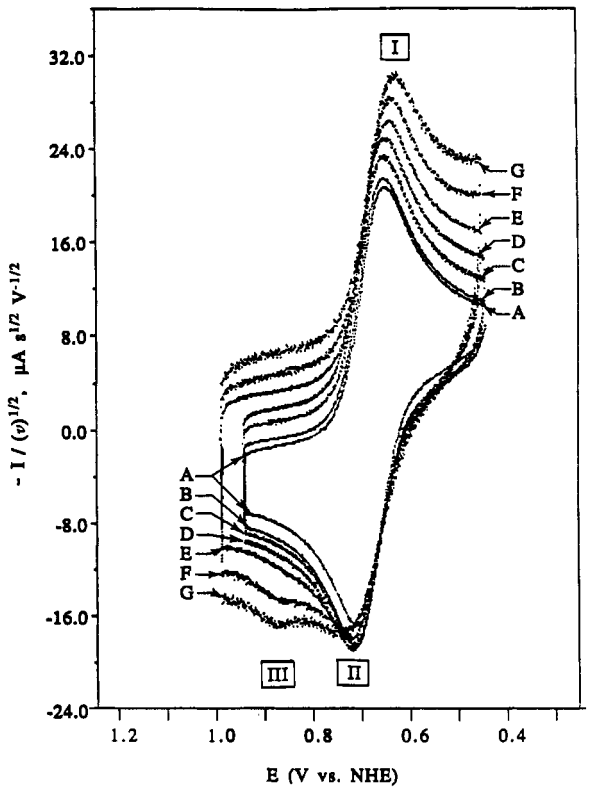

Figure 1. Slow scan cyclic voltammograms for a $Cu^{II}([14]aneS_4)$ solution in 80% methanol (0.1 M $HClO_4$, 25 °C) at a glassy carbon electrode showing the development of peak III with increasing scan rate (all scan rates in V s^{-1}): (A) 0.010, (B) 0.020, (C) 0.050, (D) 0.100, (E) 0.200, (F) 0.500, (G) 1.000 V. Reproduced with permission from ref 29. Copyright 1989 American Chemical Society.

to plate out on the electrode. All solutions were thermostated at 25 °C by circulating water from a temperature bath through a jacket placed around the electrochemical cell.

Results

The overall value of the $Cu^{II/I}L$ formal potential for an equilibrated solution of **O** and **Q** being reduced to the equilibrated reductant species, **P** and **R**, has been defined by Laviron and Roullier as E_K^f:[34]

$$\mathbf{O,Q} + e^- \rightleftharpoons \mathbf{P,R} \qquad E_K^f \tag{2}$$

This potential has previously been determined for $Cu^{II/I}([14]aneS_4)$ in 80% methanol at 25 °C, μ = 0.1 M (ClO_4^-) as E_K^f = 0.69 V (vs NHE).[29,35] The same result was obtained in this work with the glassy-carbon ultramicroelectrode at a sweep rate of 0.20 V s^{-1}, which is slow enough to result in a steady-state voltammogram.

Increasing the sweep rate in stepwise increments up to 80 000 V s^{-1} (the upper limit of our present instrumentation) generated a large number of single-sweep cyclic voltammograms both for solutions containing $Cu^{II}L$ and $Cu^{I}L$ as the initial starting species. For the time domains in which specific shifts in the positions and/or relative magnitudes of the various peaks were observed, intensive studies were conducted on the peak dependence upon sweep rate.

As can be demonstrated even with macroelectrodes for $Cu^{II}L$ solutions at 25 °C (and, more dramatically, at lower temperatures),[29] the anodic peak observed at slow scan rates, **P,R** → **O,Q** (peak II in Figure 1), begins to diminish in size with increasing scan rate as a new peak emerges at a more positive potential (peak III in Figure 1). This latter peak has previously been attributed to the direct oxidation of **R** → **Q**.[29] At the very rapid scan rates achieved with ultramicroelectrodes in the current study, this latter peak is observed to diminish in size at scan rates of 0.50 to 5.0 kV s^{-1} with the re-emergence of peak II (Figure 2) which is now shifted to a more negative potential and is attributed to the direct oxidation of **P** → **O**. This latter trend in the behavior of the anodic peaks as a function of scan rate (previously observed only at −77 °C using macroelectrodes)[29] permits the quantitative evaluation of the rate constants governing the **P**/**R** conformational interconversions, i.e., k_{PR} and k_{RP}, at 25 °C (see Discussion).

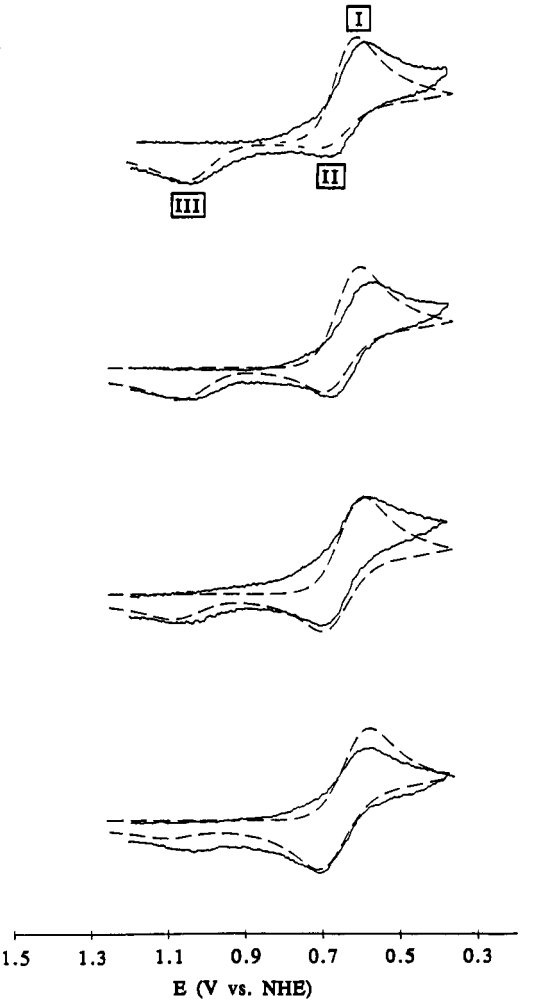

Figure 2. Rapid scan cyclic voltammograms for a 3 mM $Cu^{II}([14]aneS_4)$ solution in 80% methanol at 25 °C, μ = 1.0 M (0.33 M $Cu(ClO_4)_2$). Solid curves represent experimental CV's corrected for background while the dashed curves represent the computer simulations using the refined parameters listed in Table I. The ordinate represents current normalized for scan rate (i.e., $i/\sqrt{v}$). The electron-transfer processes associated with the individual peaks, as referenced to Scheme I, are as follows: peak I, **O** + e^- → **P**; peak II, **P** → **O** + e^-; peak III, **R** → **Q** + e^-. Scan rates (from top to bottom) are 0.5, 1.0, 2.0, and 5.0 kV s^{-1}. Peak currents for peak I (top to bottom) are 110, 150, 160, and 325 nA.

Since the heterogeneous reaction of **O** ⇌ **P** is relatively unaffected by the homogeneous reaction at 5 kV s^{-1} (corresponding to the low l/a limit[36] of cases V and VI as defined by Nicholson and Shain),[37] the midpoint between peaks I and II provides a good estimate of E_{OP}^f, the formal potential for this redox couple (see Scheme I). The resulting estimate of $E_{OP}^f \approx 0.60$ V (vs NHE) is somewhat uncertain due to the broadness of the peaks.

(34) Laviron, E.; Roullier, L. *J. Electroanal. Chem.* **1985**, *186*, 1–15.
(35) Dockal, E. R.; Jones, T. E.; Sokol, W. F.; Engerer, R. J.; Rorabacher, D. B.; Ochrymowycz, L. A. *J. Am. Chem. Soc.* **1976**, *98*, 4322–4324.
(36) The symbols l and a are used here in the same sense as defined by Nicholson and Shain[37] where $a = v(n\mathcal{F}/RT)$ and l is the sum of the forward and reverse rate constants for a first-order (or pseudo-first-order) coupled reaction (i.e., $l = k_{PR} + k_{RP}$ or $l = k_{OQ} + k_{QO}$).
(37) Nicholson, R. S.; Shain, I. *Anal. Chem.* **1964**, *36*, 706–723.

In considering the probable accuracy of the specific potential values estimated from the CV peaks, we note that errors in peak potentials may occur because of *iR* drop and current follower bandwidth limitations. Nicholson[38] and Weaver[39,40] have pointed out that large currents or uncompensated resistances can cause distortions and peak separation in the voltammogram that are indistinguishable from those due to a small heterogeneous rate constant. In the present study, the cell resistance was estimated to be 5 kΩ, which indicates that as much as 200 nA of current may be passed through the cell with a potential error of only 1 mV. The total cell current passed for the 5 kV s^{-1} scan was about 395 nA, which means that the potential control error was at most 2 mV at the peak. This was considered acceptable and would not cause significant error in the peak separation measurements and, hence, in the estimation of the heterogeneous rate constant. The operational amplifier (Burr Brown 3554) and feedback resistance used in the current follower are similar to those used by Saveant[41] for which he found a peak shift of approximately 4 mV at a scan rate of 100 kV s^{-1} using a 5-μm gold ultramicrodisk. We conclude that the error in measuring the peak potentials due to these factors is no larger than 5 mV at the highest scan rates we employed.

Low-temperature studies and computer simulations had previously established[29] that the kinetics associated with the $\mathbf{O} \rightleftharpoons \mathbf{Q}$ interconversion are very fast. Therefore, CV measurements on a $Cu^{I}([14]aneS_4)$ solution were made using scan rates up to 60 kV s^{-1} in an attempt to quantify the rate constants associated with this conformational change. Since we recognized that the *iR* drop would not be negligible at these scan rates, a fraction of the current follower output was fed back to the adder/controller in the potentiostat for *iR* drop compensation.

As observed in Figure 3, the voltammogram obtained at a scan rate of 20 kV s^{-1} shows the emergence of a cathodic peak (peak IV) in the vicinity of 0.84 V (vs NHE). This peak becomes much more distinct at a scan rate of 40 kV s^{-1}. As the scan rate is increased to 60 kV s^{-1}, this peak continues to grow at the expense of peak I. This is consistent with the assignment of peak IV to the direct reduction of $\mathbf{Q} \rightarrow \mathbf{R}$ and the scan rate at which this peak begins to appear indicates that the previous 25 °C estimate[29] of $k_{QO} \approx 1 \times 10^5$ s^{-1} (crudely approximated from −77 °C studies with a number of questionable assumptions) is within the correct order of magnitude.

Discussion

Of the many voltammograms generated in this work, those reproduced in Figures 2 and 3 provide definitive evidence at a single temperature for all the peaks predicted by the mechanism illustrated in Scheme I including the appearance of a peak (peak IV) which is assignable to the direct reduction of $\mathbf{Q} \rightarrow \mathbf{R}$.[42] The positions of the two anodic and two cathodic peaks and the conditions under which they increase and/or decrease in magnitude are in accordance with the expected behavior for Scheme I[34] and provide strong evidence for the hypothesis that the electron-transfer mechanism for the $Cu^{II}/^{I}([14]aneS_4)$ system conforms to a square scheme. Moreover, the potential values for the various peaks and their observed behavior as a function of scan rate make it possible to estimate the values for all of the specific rate constants for conformational interconversions associated with this system at 25 °C. Rough estimates of the apparent heterogeneous rate constants can also be generated.

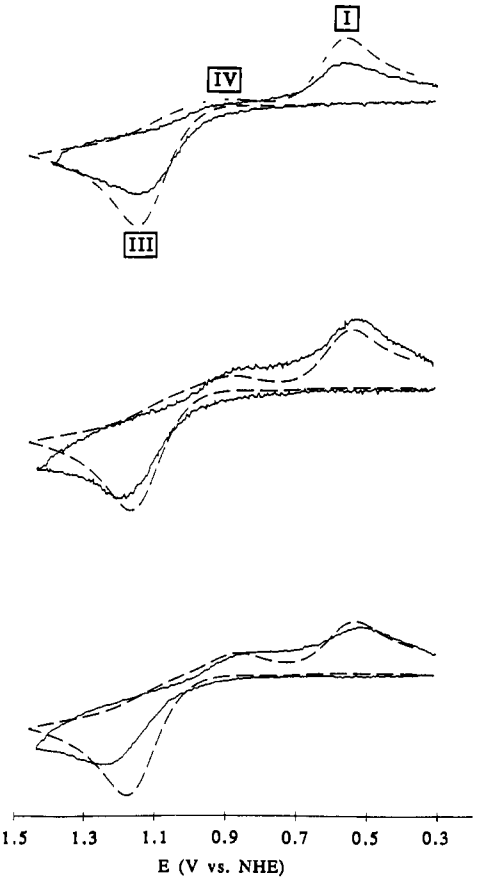

Figure 3. Rapid scan cyclic voltammograms for a 3 mM $Cu^{I}([14]aneS_4)$ solution in 80% methanol at 25 °C, $\mu = 1.0$ M ($NaNO_3$, $NaClO_4$). Solid curves represent experimental CV's corrected for background while the dashed curves represent the computer simulations using the refined parameters listed in Table I. The ordinate represents current normalized for scan rate (i.e., $i/\sqrt{v}$). The electron-transfer processes associated with the individual peaks, as referenced to Scheme I, are as follows: peak I, $\mathbf{O} + e^- \rightarrow \mathbf{P}$; peak III, $\mathbf{R} \rightarrow \mathbf{Q} + e^-$; peak IV, $\mathbf{Q} + e^- \rightarrow \mathbf{R}$. Scan rates (from top to bottom) are 20, 40, and 60 kV s^{-1}. Peak currents for peak III (top to bottom) are 640, 930, and 1260 nA.

Estimates of Heterogeneous Rate Constants. The voltammogram obtained for a $Cu^{II}L$ solution at a scan rate of 5 kV s^{-1} (Figure 2) is relatively unaffected by the homogeneous reaction, so a reasonable estimate of the heterogeneous rate constant $k_{s,OP}'$ {where the primed symbol indicates that this is an apparent (i.e., uncorrected) value} can be made by measuring the peak separation and applying Nicholson's theory for quasi-reversible reactions.[43] The value calculated in this manner is $k_{s,OP}' \approx 0.5$ cm s^{-1}.

The rate constant $k_{s,QR}'$ can not be estimated as easily from $Cu^{I}L$ voltammograms since the $\mathbf{Q} \rightarrow \mathbf{R}$ peak on the reverse scan (i.e., peak IV in Figure 3) is never completely developed even at a scan rate of 60 kV s^{-1} and the positions of the peaks may be affected by both homogeneous and heterogeneous reactions. In Nicholson and Shain's theory for the $E_{rev}C_{irr}$ electrode mechanisms[37] (which serves as a reasonable model for the $\mathbf{R} \rightarrow \mathbf{Q}$ peak), the peak on the forward scan (peak III) should be shifting towards the $E_{1/2}$ value of the electrode couple at 30 mV per decade increase in scan rate. This behavior was previously observed at lower temperature.[44] At the point that the peak for the product of the electrode reaction becomes visible on the reverse scan (peak IV), the homogeneous reaction ceases to influence the peak shift. Any subsequent peak separation is due to the slow kinetics of the electrode reaction. If we can consider 20 kV s^{-1} to represent the

(38) Nicholson, R. S. *Anal. Chem.* **1966**, *38*, 1406.
(39) Safford, L. K.; Weaver, M. J. *J. Electroanal. Chem.* **1989**, *261*, 241–247.
(40) Milner, D. F.; Weaver, M. J. *Anal. Chim. Acta* **1987**, *198*, 245–257.
(41) Garreau, D.; Hapiot, P.; Saveant, J.-M. *J. Electroanal. Chem.* **1989**, *272*, 1–16.
(42) Although peak IV never becomes truly dominant on the reduction half cycle, even at 80 kV s^{-1}, its consistent appearance under a wide variety of conditions (including slow scan measurements at −77 °C) provides strong support for the conclusion that this peak is not merely due to experimental anomaly or invalid background corrections.
(43) Nicholson, R. S. *Anal. Chem.* **1965**, *37*, 667–671; 1351–1355.
(44) See ref 29, Figure 2, curves B and C; for additional examples, see: Bernardo, M. M. Ph.D. Dissertation, Wayne State University: Detroit, MI, 1987.

approximate point where this process begins (Figure 3), then the 30-mV shift from 20 to 40 kV s^{-1} is compatible with a heterogeneous rate constant of $k_{s,QR}' \approx 0.1$ cm s^{-1}.[43] Since these data may be distorted by iR drop, the positions of the peaks on the reverse scan of the $Cu^{II}L$ system can serve as a check on this rate constant. From computer simulations, it is apparent that a variation of the heterogeneous rate constant value from 0.5 to 0.1 cm s^{-1} results in a difference in the peak position of 300–400 mV; the actual separation of these peaks is about 340 mV, which suggests that a value of $k_{s,QR}' \approx 0.3$ cm s^{-1} could apply.

Evaluation of Conformational Equilibrium Constants. As noted in the Results section, the positions of peaks I and II for a Cu^{II}([14]aneS$_4$) solution at a scan rate of 5 kV s^{-1} (Figure 2) yields $E_{OP}^f \approx 0.60$ V (vs NHE). As shown by Laviron and Roullier,[34] the microscopic potentials in the square scheme are related to the overall thermodynamic potential, E_K^f, by the following relationships:

$$E_{OP}^f = E_K^f - (RT/n\mathcal{F}) \ln [(1 + K_{PR})/(1 + K_{OQ})] \quad (3)$$

$$E_{QR}^f = E_K^f - (RT/n\mathcal{F}) \ln [(1 + K_{PR}^{-1})/(1 + K_{OQ}^{-1})] \quad (4)$$

Recognizing that $K_{OQ} \ll 1$ (vide infra), substitution of $E_{OP}^f = 0.60$ V and $E_K^f = 0.69$ V into eq 3 yields a value of $K_{PR} \approx 32$ for the equilibrium between the two Cu^IL species. This value of K_{PR} should be reflected in the relative magnitude of peaks II and III for a Cu^IL solution when $l_{RP}/a \ll 1$ (where $l_{RP} = k_{RP} + k_{PR}$). As revealed in Figure 3, peak II is virtually undetectable for a Cu^IL solution at very rapid scan rates. Based on the degree of resolution for the voltammograms in Figure 3, this observation provides independent evidence that $K_{PR} \geq 30$.

A crude estimate of the $E_{1/2}$ value based on the positions of peaks III and IV (Figure 3) suggests that $E_{QR}^f \leq 1.01$ V (vs NHE). Substituting this value into eq 4 yields $K_{OQ} \geq 4 \times 10^{-6}$. The uncertainty in this value is due to the inability to identify accurately the position of the peak maximum for peak IV which may be further complicated by the distortions caused by iR drop and the quasi-reversibility discussed earlier.

Evaluation of Conformational Rate Constants. Using the peak current ratio for peaks II and III, the magnitude of the rate constant for the conversion of $\mathbf{P} \rightarrow \mathbf{R}$, *i.e.*, k_{PR}, can be estimated from Nicholson's semiempirical method[38] and from Nicholson and Shain's graphical data for the $E_{rev}C_{irr}$ case (Case VI).[37] This approach yields $k_{PR} \approx 2 \times 10^3$ s^{-1}, from which we then estimate that $k_{RP} \approx 60$ s^{-1} (assuming $K_{PR} \approx 32$). Using Nicholson and Shain's Case III for $C_{rev}E_{rev}$, the current ratios at slower scan rates for peaks I and II for a Cu^IL solution yield an independent estimate of $35 \leq k_{RP} \leq 90$ s^{-1}. Since the methods used assume reversibility of the electrode reactions, they cannot be considered highly accurate. The resulting estimates of these two rate constants are within about an order of magnitude of the 25 °C values we estimated previously[29] ($k_{PR} \approx 10^4$ s^{-1}, $k_{RP} \approx 10^3$ s^{-1}) from the variable temperature data, and we note that these latter values have been corroborated in the simulations of our earlier data as performed by Lerke, Evans and Feldberg.[45] In this context, it should be reemphasized, however, that the previous estimates were inexact since they were based on behavior observed at low temperature (0 to −77 °C), and the lack of knowledge of the temperature dependencies prevented accurate extrapolations to 25 °C.

For Cu^IL solutions, it is obvious from Figure 3 that, even at a scan rate of 60 kV s^{-1}, peak IV has not become dominant. For an $E_{rev}C_{irr}$ system (Nicholson and Shain's Case VI),[37] the peak current ratio for peaks III and IV at scan rates of both 40 and 60 kV s^{-1} yields an estimated value of $k_{OQ} \approx 4 \times 10^5$ s^{-1}. If we use our estimate of $K_{OQ} \geq 4 \times 10^{-6}$, we then estimate $k_{OQ} \geq 2$ s^{-1}. In selecting these latter values, it should be noted that the actual values of K_{OQ} and k_{OQ} have no influence on the *shape* of the voltammogram as long as K_{OQ} is large. However, the value of K_{OQ} does shift the *position* of peaks III and IV due to its effect on the reduction potential, E_{QR}^f (eq 4).

Table I. Estimated Parameters for the $Cu^{II/I}$([14]aneS$_4$) Redox Couple in 80% Methanol at 25 °C, μ = 1 M (All Parameters Referenced to Scheme I).

parameter	initial estimates (rapid scan CV)	refined estimates (computer simulation)
E_{OR}^f, V	0.69[a,b]	0.69[a]
E_{OP}^f, V	0.60[a]	0.59[a]
E_{QR}^f, V	≤1.01[a]	0.95[a]
$k_{s,OP}$, cm s^{-1}	0.5	0.5
$k_{s,QR}$, cm s^{-1}	0.1–0.3	≈0.2
K_{PR}	32	50
K_{OQ}	$\geq 4 \times 10^{-6}$	4×10^{-5}
k_{PR}, s^{-1}	2×10^3	3×10^3
k_{RP}, s^{-1}	60 (35–90)	60
k_{OQ}, s^{-1}	≥2	5
k_{QO}, s^{-1}	4×10^5	1.2×10^5

[a] All potential values vs NHE (based on E^f = 0.197 V for Ag/AgCl reference electrode). [b] As determined from static and slow scan measurements: Bernardo, M. M.; Schroeder, R. R.; Rorabacher, D. B. *Inorg. Chem.* **1991**, *30*, 1241–1247. Cf. refs 29 and 35.

Computer Simulations of the Cyclic Voltammograms. To obtain improved evaluations of the rate constants representing the various conformational changes, computer simulations were made to determine the values which would permit a reasonable duplication of the observed voltammograms at these rapid scan rates. The simulation approach used was a modification of that developed by Feldberg.[46] In our approach, integrated rate equations were used to establish the concentrations of the reactants and products of homogeneous chemical reactions. This approach forfeits some of the generality normally sought in digital simulation; however, such generality is not required in our case.

The simulation parameters included E_{OR}^f, k_{OQ}, k_{QO}, k_{PR}, k_{RP}, α (0.5 in all cases), $k_{s,OP}'$, and $k_{s,QR}'$. All diffusion coefficients were assumed to be 1.0×10^{-5} cm^2 s^{-1}.[47] The homogeneous reaction parameters were varied so the simulations would match the positions and relative heights of the experimentally measured voltammetric peaks. The heterogeneous rate constants were then adjusted to reproduce the appropriate separations in the cathodic and anodic waves. The selection of the homogeneous reaction parameters was of greatest importance and considerable effort was made to match these values as closely as possible. The heterogeneous parameters obtained from the simulations are only approximate and no attempt to refine these values beyond a few iterations was deemed worthwhile, both from their secondary importance and from their method of calculation in the simulation. At each potential the simulation program calculated the forward and reverse rate constants from the Butler–Volmer equation using k_s, α, E_K^f, and E. Since the simulation calculations did not include parameters such as double layer capacitance, point of zero charge, or ionic strength, the k_s values are only uncorrected estimates of the heterogeneous rate constants.

The individual simulation parameters were changed sequentially on a trial and error basis starting with the initial estimates outlined above as tabulated in Table I. Due to the extremely large background corrections, the actual magnitudes of the

(45) Lerke, S. A.; Evans, D. H.; Feldberg, S. W. *J. Electroanal. Chem.* **1990**, *296*, 299–315 (n.b. p 310).

(46) (a) Feldberg, S. W. *Electroanal. Chem.* **1969**, *3*, 199–296. (b) Feldberg, S. W. *Comput. Chem. Instrum.* **1972**, *2*, 185–215.

(47) From the steady-state voltammogram, a value of $D = 5.0 \times 10^{-6}$ cm^2 s^{-1} was calculated using the steady-state condition, $i = n\ sc\pi^{1/2}ADbC$, assuming $b = 2.257$ and an electrode radius of 5 μm (J. Heinze, *J. Electroanal. Chem.* **1981**, *124*, 73–86). However, due to the large background corrections, the actual amplitude of the corrected currents was not judged to be highly accurate, and only the relative peak heights, rather than their absolute magnitudes, were considered significant in simulating the experimental voltammograms. Thus, the actual value of the diffusion coefficient itself was of no consequence in the data analysis.

individual peaks were not deemed to be highly accurate and only the relative peak heights as well as the peak positions were emphasized in simulating the experimental voltammograms. Fitting of the homogeneous parameters went smoothly, and only a few iterations were needed to move from the initial estimates to our final values. We did not attempt to obtain an exact match for any specific voltammogram but, rather, ensured that the simulations showed the same relative trends with scan rate as those observed in our experiments. The errors in the final match between the simulated and experimental curves are attributed to the limits of accuracy arising from the large background correction.

The major difficulty proved to be the reproduction of peaks III (representing $\mathbf{R} \rightarrow \mathbf{Q}$) and IV (representing $\mathbf{Q} \rightarrow \mathbf{R}$) since these peaks are obviously affected not only by homogeneous reactions but also by the quasireversible nature of the electrode process. In simulating high scan rates, such as those needed to produce peak IV in experimental voltammograms, the simplicity of the heterogeneous rate constant calculations precluded accurate matching of the simulated and experimental peaks.

Using $k_{s,QR}' = 0.1$ cm s^{-1}, but otherwise applying the parameters given in Table I, we obtained an excellent match for the Cu^{I}L data at a scan rate of 20 kV s^{-1}. However, at scan rates of 40 and 60 kV s^{-1}, the simulations showed a larger peak shift for peaks III and IV than that due to the heterogeneous rate constant, and peak III was also shifted to potentials which were too positive as the scan rate increased. When $k_{s,QR}'$ was increased to 0.3 cm s^{-1}, the reproduction of peak III was improved for the Cu^{II}L data but the reproduction of peak IV (Figure 2) was shifted in a positive direction relative to the experimental peak for the Cu^{I}L data (Figure 3). The final simulations were based on a compromised value of $k_{s,QR}' = 0.2$ cm s^{-1}. As illustrated by the dashed curves in Figures 2 and 3, these simulations approximate the experimental results.

The refined parameters used are given in the right-hand column of Table I. In all cases, these values are within about an order of magnitude of the 25 °C values estimated previously from the variable-temperature data.[29] It should be emphasized, however, that the value of the equilibrium constant K_{OQ} is not considered highly accurate since the observed shift in the positions of peaks III and IV at high scan rates can result from either the heterogeneous rate constant $k_{s,QR}'$ or the equilibrium constant K_{OQ}. As noted above, changes in the values of k_{OQ} and K_{OQ} have little effect on the shape of the voltammograms provided that the latter equilibrium constant is very large and that Nicholson's l/a parameter is also large. Thus, there is considerable latitude in estimating the value of k_{OQ}, presently assigned a value of 5 s^{-1}. All other rate constant values for conformational interconversions are considered to be accurate within a factor of about 3–10.

Nature of Conformational Changes. In previous crystal structural determinations, we have noted that Cu^{II}([14]aneS$_4$)[48] involves the planar coordination of all four thiaether sulfur donor atoms to the Cu(II) with long axial bonds to two perchlorate anions to complete a well-defined tetragonal coordination geometry. In solution, it is presumed that the axial sites in species **O** are replaced by solvent molecules. A crystal structure determination of Cu^{I}([14]aneS$_4$) revealed a tetrahedral coordination geometry for Cu(I) in which one Cu–S coordinate bond was ruptured with the fourth coordination site occupied by a sulfur from an adjacent ligand to generate a polymeric chain.[49] However, the solution behavior of the Cu^{I}L species shows no evidence for the presence of polymeric species,[29] and we note that a recent crystal structure for the closely related Cu^{I}([14]aneNS$_3$) complex (in which one sulfur donor atom is replaced by an amine nitrogen) has revealed a flattened tetrahedral geometry in which all four donor atoms from the same ligand are coordinated to a single copper atom.[50] Molecular models suggest that the latter geometry is easily accessible for Cu^{I}([14]aneS$_4$) as well, and this geometry probably prevails for species **R** in solution.

Although the coordination geometries of the two metastable intermediates have not yet been identified, we suggest that **P** is conformationally related to **O** and **Q** is conformationally related to **R** as has been suggested in the general theoretical treatment for electron-transfer square schemes involving conformational change.[11] In support of this hypothesis, we note that Meyerstein and co-workers[51] have found, in a pulse radiolytic study, that the reduction of Cu^{II}(Me$_6$[14]dieneN$_4$) by hydrated electrons generates a planar Cu^{I}L product which then becomes equilibrated with a second Cu^{I}L species (presumed to be tetrahedral), the latter species being identical to the product of normal electrochemical reduction. Since the axial solvent molecules are held only loosely in species **O**,[48] we presume that the primary contribution to the energy barrier for the $\mathbf{P} \rightleftharpoons \mathbf{R}$ and $\mathbf{O} \rightleftharpoons \mathbf{Q}$ interconversions is the inversion of two coordinated sulfur atoms and the accompanying eclipsing of hydrogens in the alkyl bridges required to convert the tetragonal conformer to the tetrahedral conformer.[50]

Correlations to Cross Reactions. From the magnitude of the values estimated for the conformational equilibrium constants, K_{OQ} and K_{PR}, it is obvious that the intermediate species designated as **P** is much more stable than the intermediate **Q** relative to their respective stable conformers. Thus, for cross reactions (reaction 1) *run under conditions where all species are completely equilibrated*, pathway $\mathbf{O} \rightleftharpoons \mathbf{P} \rightleftharpoons \mathbf{R}$ (designated previously as pathway A)[29] should predominate over pathway $\mathbf{O} \rightleftharpoons \mathbf{Q} \rightleftharpoons \mathbf{R}$ (pathway B) for processes involving either the oxidation or reduction of Cu$^{II/I}$([14]aneS$_4$).

Each of the two pathways should exhibit its own characteristic self-exchange rate constant:

$$*\mathbf{O} + \mathbf{P} \rightleftharpoons *\mathbf{P} + \mathbf{O} \qquad k_{AA} \tag{5}$$

$$*\mathbf{Q} + \mathbf{R} \rightleftharpoons *\mathbf{R} + \mathbf{Q} \qquad k_{BB} \tag{6}$$

These homogeneous electron self-exchange rate constants should correlate to the two heterogeneous rate constants, $k_{s,OP}$ and $k_{s,QR}$, respectively, according to the relationship developed by Marcus[52]

$$\frac{k_s}{Z_{el}} = \sqrt{\frac{k_{ii}}{Z}} \tag{7}$$

where $Z_{el} \approx 10^4$ cm s^{-1} is the frequency factor for the heterogeneous reactions at an electrode, $Z \approx 10^{11}$ M^{-1} s^{-1} represents the corresponding frequency factor for encounters between reactants in the homogeneous cross reactions, and k_{ii} represents k_{AA} or k_{BB}.

Equation 7 applies to the work-corrected rate constants,[52] whereas the $k_{s,OP}'$ and $k_{s,QR}'$ values estimated in this study are "apparent heterogeneous rate constants" (not corrected for double layer effects). The correction to true standard rate constants would require knowledge of the point of zero charge and the double layer capacitance.[53,54] Such parameters cannot readily be obtained for the complex solutions used in this work; moreover, it is not evident that estimated standard parameters would add to the significance of the results. However, it is clear that, in the potential range of our studies, the electrode surface is positively

(48) Glick, M. D.; Gavel, D. P.; Diaddario, L. L.; Rorabacher, D. B. *Inorg. Chem.* **1976**, *15*, 1190–1193.
(49) Diaddario, L. L., Jr.; Dockal, E. R.; Glick, M. D.; Ochrymowycz, L. A.; Rorabacher, D. B. *Inorg. Chem.* **1985**, *24*, 356–363.
(50) Bernardo, M. M.; Heeg, M. J.; Schroeder, R. R.; Ochrymowycz, L. A.; Rorabacher, D. B. *Inorg. Chem.* **1992**, *31*, 191–198.
(51) Freiberg, M.; Lilie, J.; Meyerstein, D. *Inorg. Chem.* **1980**, *19*, 1908–1912; the ligand Me$_6$[14]dieneN$_4$ represents 5,7,7,12,14,14-hexamethyl-1,4,8,11-tetraazacyclotetradeca-4,11-diene.
(52) Marcus, R. A. *J. Chem. Phys.* **1965**, *43*, 679–701.
(53) Bard, A. J.; Faulkner, L. R. *Electrochemical Methods: Fundamentals and Applications*; Wiley: New York, 1980; p 543–544.
(54) For carbon electrodes, the point of zero charge at the surface lies between −0.07 and +0.02 V (vs NHE): *Encyclopedia of Electrochemistry*; Hampel, C. A., Ed.; Reinhold: New York, 1964; pp 776–778.

charged.[54] Therefore, the apparent heterogeneous rate constants estimated from our measurements ($k_{s,OP}' \approx 0.5$ cm s^{-1} and $k_{s,QR}' \approx 0.2$ cm s^{-1}) are obviously lower than the standard values.

In independent measurements using NMR line-broadening on the $Cu^{II/I}$([14]aneS$_4$) system, we have obtained a rate constant of $k_{11} = 8 \times 10^3$ M^{-1} s^{-1} at 25 °C for the overall **O,R** electron self-exchange.[32] On the basis of the data obtained in the current study, this value should represent electron exchange via pathway A (designated as $k_{11(A)}$) since, as noted above, the **P** intermediate is much more stable than the **Q** intermediate. Thus, the specific rate constant for the **O,P** self-exchange, k_{AA} (reaction 5), can be estimated from the value obtained from the NMR measurements using the K_{PR} value generated in the current investigation:

$$k_{AA} = K_{PR}k_{11(A)} \approx 50 \times 8 \times 10^3 \text{ M}^{-1} \text{ s}^{-1} = 4 \times 10^5 \text{ M}^{-1} \text{ s}^{-1}$$

Substitution of this k_{AA} value into eq 7 then results in an estimate of the standard value of the hetereogeneous rate constant of $k_{s,OP} \approx 20$ cm s^{-1}. The implied correction to the apparent heterogeneous rate constant, $k_{s,OP}'$ (Table I), appears reasonable.

Applying similar logic for pathway B, we assume that the rough estimate of $k_{s,QR}' \approx 0.2$ cm s^{-1}, as generated in this work, would then be equivalent to a standard value of $k_{s,QR} \approx 8$ cm s^{-1}. The latter estimate then yields $k_{BB} \approx 7 \times 10^4$ M^{-1} s^{-1} using eq 7. This value can then be used to provide a crude estimate of the overall self-exchange rate constant via pathway B:

$$k_{11(B)} = k_{BB}K_{OQ} \approx 7 \times 10^4 \text{ M}^{-1} \text{ s}^{-1} \times 4 \times 10^{-5} \approx 3 \text{ M}^{-1} \text{ s}^{-1}$$

For homogeneous reactions involving the *oxidation* of Cu^I([14]aneS$_4$) by a suitable counter reagent, A_{Ox}, as shown in reaction 1, the results of our electrochemical studies indicate that whereas pathway A is the preferred reaction pathway, the rate constant for the conformational conversion of **R** → **P** (i.e., k_{RP}) ultimately limits how fast the overall reaction can go by this (i.e., **R** → **P** → **O**) pathway. Our estimate of $k_{RP} \approx 60$ s^{-1} defines the characteristic first-order rate constant which should govern the appearance of "gated" electron transfer[11,13] with this system in 80% methanol at 25 °C. This value appears to be in excellent agreement with a value independently obtained from cross reaction studies in aqueous solution; i.e., $k_{RP} = 50 \pm 10$ s^{-1}.[32] Moreover, application of the Marcus relationship to the overall rate constants for homogeneous oxidation cross reactions (in aqueous solution) which appear to have exceeded this rate constant for conformational change yield apparent values for the self-exchange rate constants in the range of $k_{11} = 0.4$–1.6 M^{-1} s^{-1}, in close agreement with our estimate of $k_{11(B)} \approx 3$ M^{-1} s^{-1} as given above.

For reactions conducted in aqueous solution, some variation in k_{RP} may occur as a result of solvent effects, but the aqueous value is expected to lie within the same order of magnitude since an intramolecular rearrangement is involved (although one or two loosely-coordinated solvent molecules may enter the inner-coordination sphere in converting species **R** to **P**). Therefore, we can predict that as counter reagents having larger self-exchange rate constants and/or higher potential values are selected for reaction 1, the reaction half-life is expected to decrease until it approaches the half-life of **R** → **P** (≈ 10 ms). With this estimate in hand, the range of conditions under which we may expect to observe "gated" electron-transfer behavior in oxidation reactions involving Cu^I([14]aneS$_4$) is now evident. This behavior has been definitively demonstrated in our recent cross-reaction study.[32]

Acknowledgment. The authors wish to thank Professor Leo A. Ochrymowycz of the University of Wisconsin—Eau Claire for providing the sample of [14]aneS$_4$. The assistance of Brian Dunn in generating the final computer simulations is also gratefully acknowledged.